SANDIA REPORT

SAND92—1275 • UC—721
Unlimited Release
Printed August 1992

Thermal Diffusion Processes in Aqueous Sodium Chloride Solutions

Randall T. Cygan, Glenn D. Jarrell

Prepared by
Sandia National Laboratories
Albuquerque, New Mexico 87185 and Livermore, California 94550
for the United States Department of Energy
under Contract DE-AC04-76DP00789

Issued by Sandia National Laboratories, operated for the United States Department of Energy by Sandia Corporation.

Available to DOE and DOE contractors from
Office of Scientific and Technical Information
PO Box 62
Oak Ridge, TN 37831

Prices available from (615) 576-8401, FTS 626-8401

Available to the public from
National Technical Information Service
US Department of Commerce
5285 Port Royal Rd
Springfield, VA 22161

NTIS price codes
Printed copy: A03
Microfiche copy: A01

Distribution

Category UC-721

SAND92-1275

Unlimited Release

Printed August 18, 1992

THERMAL DIFFUSION PROCESSES IN AQUEOUS SODIUM CHLORIDE SOLUTIONS

Randall T. Cygan

Geochemistry Department 6118
Sandia National Laboratories
Albuquerque, NM 87185

and

Glenn D. Jarrell

ManTech Environmental Technology Inc.
Corvallis, OR 87333

ABSTRACT

Thermal diffusion, or Soret diffusion, has been suggested as an overlooked mechanism for mass transfer in a variety of geological environments. However, when experimental data are available, the mass transport of a chemical component in response to a thermal gradient (that is, the Soret effect) is usually found to be insignificant in comparison to other mass transfer processes, such as fluid convection or isothermal diffusion. Nonetheless, the thermal diffusion process is the primary and critical driving force for the migration of fluid inclusions in rocksalt deposits. A detailed evaluation of the magnitude of the Soret rate constants is critical in modeling the migration of fluid inclusions up the thermal gradient associated with a radioactive waste repository. Thermal diffusion may lead to the eventual corrosion of waste canisters and the leaching of radioisotopes from the waste forms, resulting in the introduction of these contaminants into the environment.

Several analytical models provide approximations to the exact solution of the fundamental partial differential equation which describes the thermal diffusion process in a finite cell with fixed boundary temperatures. An implicit central difference numerical model indicates that the time dependency of an evolving thermal profile towards its linear steady state profile may introduce a reversal in the usual Soret signature of a chemical system. These transient effects are small and occur during the very early stages of the process when the nonlinear temperature profile is most extreme. All of the models predict an eventual steady state compositional profile that is linear across the length of the cell and results when the mass flux of thermal diffusion equals the opposing flux associated with isothermal diffusion.

An experimental conductimetric technique provides a unique method for examining the thermal diffusion process for aqueous NaCl solutions. The ratio of half-cell solution conductances, for a Soret Cell with an externally imposed thermal gradient, is monitored as a function of time. Soret coefficients and isothermal diffusion coefficients for the NaCl solutions are simultaneously determined based upon the best fit of the models to the observed conductance (concentration) ratios. Soret coefficients at mean temperatures of 40°C and

50°C and at thermal gradients of 10°/cm and 20°/cm were determined. The Soret coefficients range from 1.05 /deg to 2.50 /deg at 40°C and from 2.05 /deg to 4.20 /deg at 50°C for NaCl solution concentrations of 0.1 N to 1.0 N. The Soret coefficients appear to be independent of the magnitude of the thermal gradient, and not a strong function of temperature as normally observed for isothermal diffusion coefficients.

TABLE OF CONTENTS

LIST OF FIGURES

LIST OF TABLES

ACKNOWLEDGMENTS

We would like to acknowledge the careful reviews provided by Henry Westrich and David Zeuch. William Casey, Carol Stein, and James Krumhansl provided comments and advice during the course of the research and reviewed an early draft of the manuscript. The first author would also like to acknowledge the discussions with I-Ming Chou during the early stages of the research and his suggestions for improving upon previous experimental approaches.

INTRODUCTION

Thermal diffusion processes can be identified as the mass transport response of a system to a gradient in temperature. Although simply stated, thermal diffusion is far from being so simply understood. Both in theoretical and experimental perspectives, thermal diffusion studies are complicated by the lack of a suitable atomic theory and by the limited nature of its effect in experimental observation. Although thermal diffusion effects may result in large-scale phenomena (below), little is known of the magnitude, or for that matter, the sign of the standard thermal diffusion rate terms (Soret coefficients). In addition to the complicated nature of thermal diffusion processes themselves, recent research on this physiochemical process has been burdened by the equally complicated nomenclature introduced by researchers in their attempt to understand and evaluate the phenomena. Terms such as Soret diffusion, Ludwig effect, and thermodiffusion are synonymous with thermal diffusion, while Clusius-Dickel and thermogravitational effects describe more complicated mass transfer processes. The often-used term "Soret diffusion" will occasionally be interchanged with "thermal diffusion" in this paper.

Thermal diffusion processes have been discussed in a wide range of applications in recent years. Although the most immediate concern is for understanding the mass transport associated with the isolation of radioactive waste, thermal diffusion has been analyzed for a variety of other applications. Costeséque (1985) has examined thermal diffusion as it affects the concentration of brines associated with evolving geothermal systems. Similarly, Dickey (1966, 1969) and Bischoff and Rosenbauer (1989) have suggested this thermal effect to be a possible mechanism in enhancing brine compositions of selected subsurface waters. Thermal diffusion processes have also been examined (Schott, 1983; Carrigan and Cygan, 1986) for the case of evolving magmatic systems. Longhurst (1985) discusses the role of thermal diffusion in transport of isotopes associated with a fusion reactor, while Rothmeyer (1980) analyzes its role in enhancing the efficiency of solar ponds. Although not limited to gas and liquid phases, recent materials studies (Ghadekar and Deshmukh, 1982; Reuther, 1984; Wada *et al.*, 1985) have examined thermal diffusion effects *in* solids. Historically, though, the most intense research (for example, Jones and Furry, 1946) was devoted to the examination of thermal diffusion of gases

for the enrichment of uranium isotopes to be used for nuclear weapons in the Manhattan Project.

Recent theoretical studies of nuclear waste repositories have concentrated on the coupling of heat flow, stress, mass transport, and chemical reaction (Krause and Loken, 1981; Tsang *et al.*, 1983; Carnahan, 1984). However, estimates of thermal diffusion effects have been largely speculative. Recently, Seyfried and Thornton (1982) and Thornton and Seyfried (1983) were able to experimentally derive Soret coefficients for fluids associated with seabed sediments. Although transport induced by the applied temperature gradients was limited, these studies were the first to evaluate high temperature data for radioactive waste applications.

For the analysis of radioactive waste in rocksalt repositories, no suitable data base of Soret data exists. Most of the original experimental studies were restricted to low temperatures and solutions of low ionic strength (for example, Agar, 1960; Agar and Turner, 1960). Jenks (1979) and Jenks and Claiborne (1981) discuss the significance of thermal gradients in salt and the related implications for disposal of nuclear wastes. One of the primary concerns in the rocksalt repositories, primarily for bedded rocksalt formations, is the effect of fluid inclusion migration (Chou, 1982a; Olander *et al.*, 1982; Pigford, 1982). Roedder and Belkin (1980) have provided experimental data for the behavior of brine-filled fluid inclusions in response to a thermal gradient. Figure 1 provides photomicrographs of one of their migrating inclusions under conditions expected at a waste repository. Normally, these fluid inclusions migrate up the temperature gradient as NaCl is dissolved at the hot end and reprecipitated at the cold end. Thermal diffusion provides the mechanism for mass transport across the static fluid of the inclusion. Theoretical analyses (Chou, 1982a; Olander *et al.*, 1982) emphasize the role of temperature, thermal gradient, and fluid inclusion size in the migration of the brine inclusions. However, the most unknown critical factor in such analysis is that of the Soret coefficient. Figures 2 and 3 provide the results of Chou (1982b) in which inclusion migration limits are given as a function of the Soret coefficient σ. Figure 2 provides the evaluation of migration in an infinite halite crystal while Figure 3 denotes the case of inclusion migration across a grain boundary and the effect of the additional energy barrier at the interface. The expected conditions for fluid inclusions at the Waste

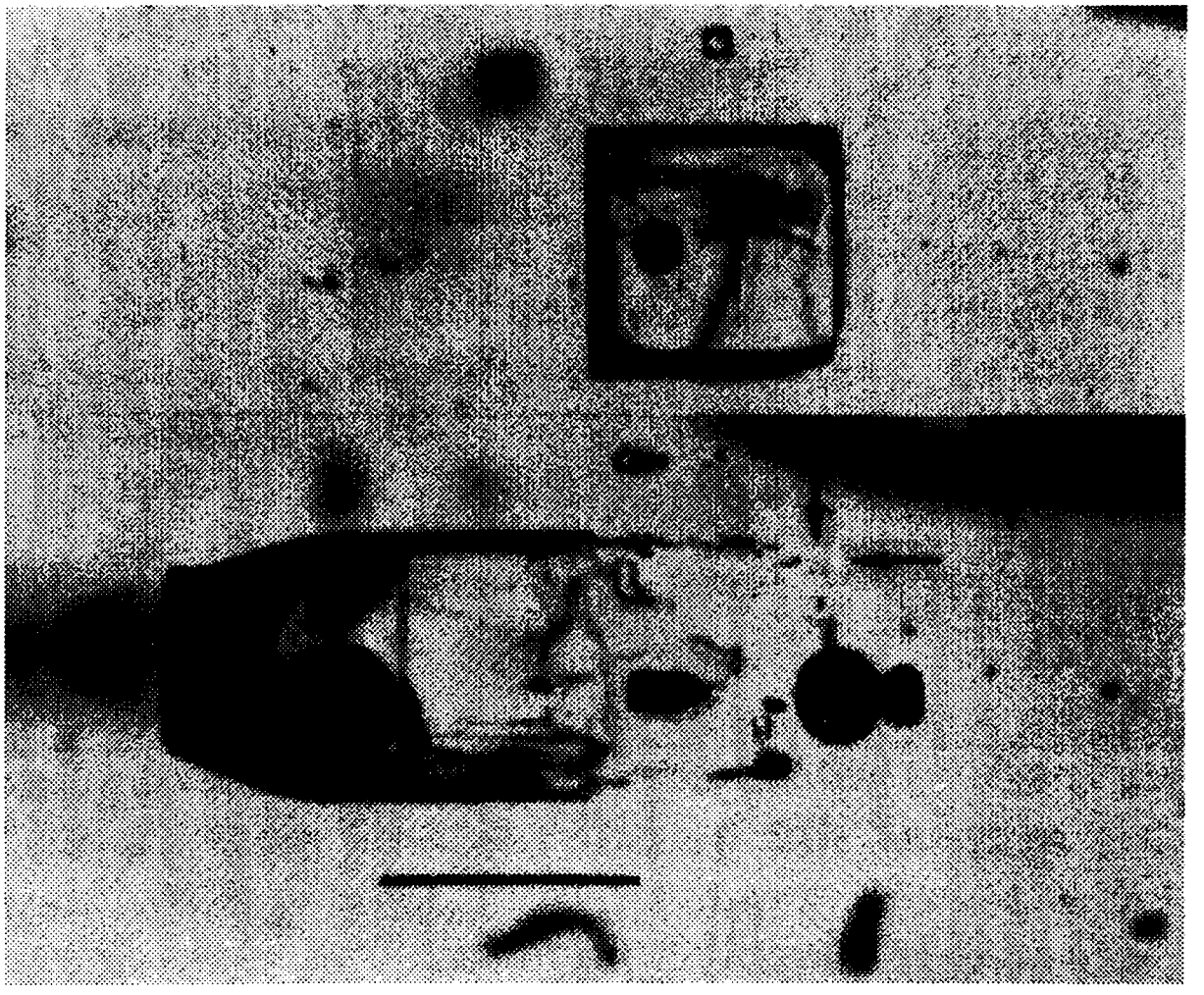

Figure 1. Photomicrograph of fluid inclusion in rocksalt from Waste Isolation Pilot Plant, Carlsbad, New Mexico, before (upper) and after (lower) heating with an imposed thermal gradient of 1.5°C/cm at 202°C for 156 hours. The arrows denote the original boundary of the fluid inclusion. The scale bar represents a distance of 500 μm. From Roedder and Belkin (1980).

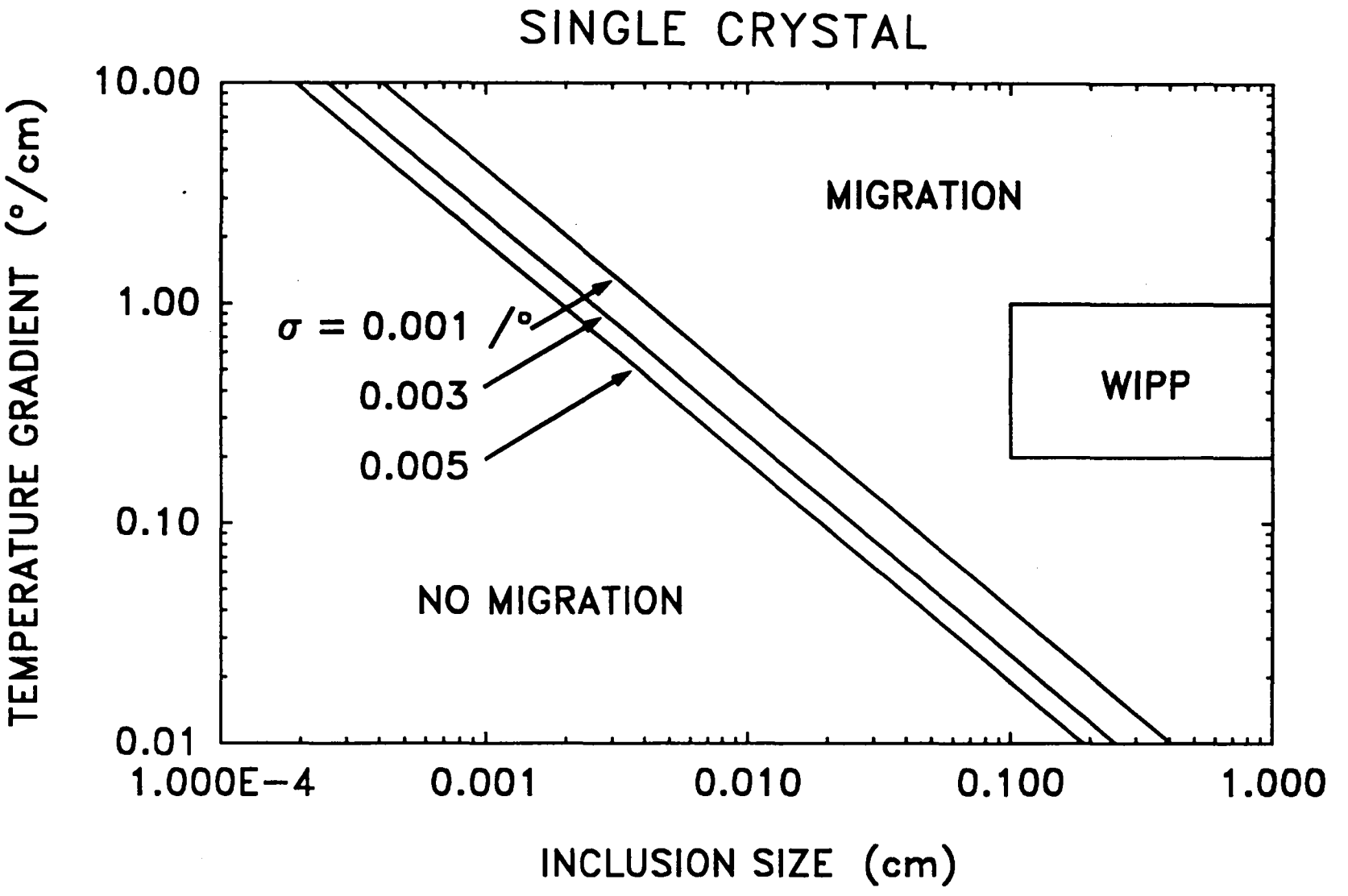

Figure 2. Threshold migration limits for fluid inclusion migration in an infinitely large halite crystal for a fluid composition of 2.41 m $MgCl_2$ as a function of Soret coefficient σ, thermal gradient, and inclusion size. Expected conditions for the Waste Isolation Pilot Plant are denoted. From Chou (1982b).

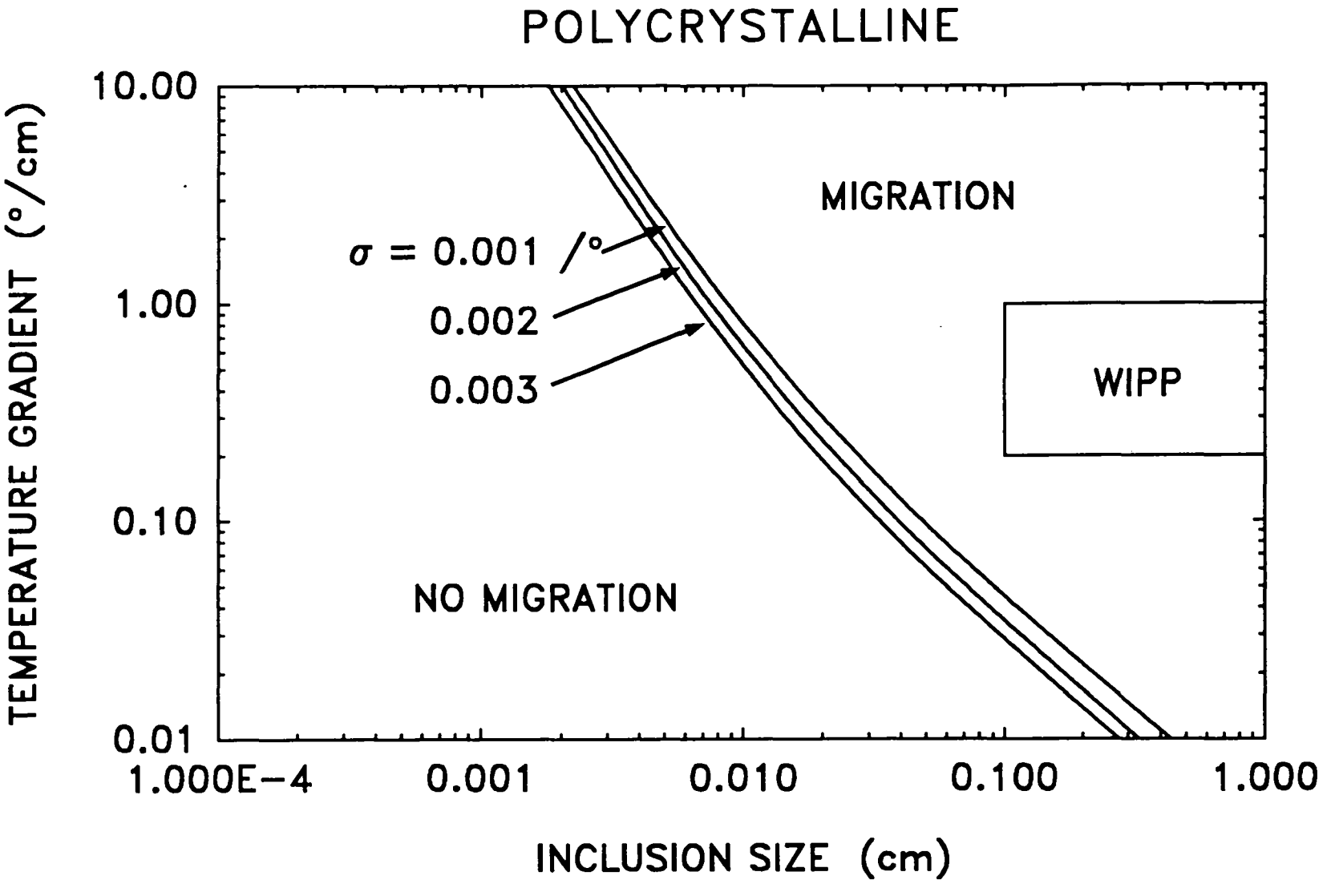

Figure 3. Threshold limits for fluid inclusion migration across grain boundaries in a polycrystalline halite sample for a fluid composition of 2.41 m $MgCl_2$ as a function of Soret coefficient σ, thermal gradient, and inclusion size. Expected conditions for the Waste Isolation Pilot Plant are denoted. From Chou (1982b).

Isolation Pilot Plant at Carlsbad, New Mexico are denoted; however, much higher transient temperature gradients can be expected in the very near-field environment of the waste canisters.

The present study was initiated to examine the behavior of mass transport in the NaCl-H_2O system as influenced by a thermal gradient. By an examination of this particular chemical system, the results of this effort should contribute an evaluation of the role of thermal diffusion processes in the isolation of radioactive wastes in an underground rocksalt repository. An analysis is made of the previous experimental research and the suitability of these data for application to the conditions of the waste repository. The results of recent experimental determinations of Soret coefficients in this system at more applicable temperatures are also presented and evaluated in light of these previous studies. A discussion of the fundamental phenomenological theory is first presented along with a numerical evaluation of the thermal diffusion response of aqueous solutions in a Soret cell. A review of previous experimental studies is presented along with a detailed description of the Soret cells used in the present study and a discussion of the experimental method. The final section provides a discussion of the Soret results and their application.

THEORY

A phenomenological approach has traditionally been used to examine thermal diffusion processes. Little understanding exists of the microscopic behavior of chemical species under the influence of a temperature gradient, although recent experimental studies (Chanu, 1967; Yow *et al.*, 1977) have provided information on the entropy of transfer and the structure of solutes in solution (Denbigh, 1952). The following discussion provides the basic rudiments of the phenomenological theory as originally developed by Furry *et al.* (1939) and DeGroot (1947) and later extended by Agar (1960) and DeGroot and Mazur (1962). Excellent reviews and details for application to liquids and aqueous solutions are provided by Mizushina and Ito (1963) and Powers (1962).

The principal premise of irreversible thermodynamics states that the rate of entropy production must always be greater than zero for a nonequilibrium system. This rate is related to the sum of the products of fluxes and forces. The flux J_i for the transfer of a process component (for example, mass or heat) is given by:

$$J_i = \sum_j L_{ij} X_j \tag{1}$$

L_{ij} are the phenomenological coefficients which can be related to the macroscopic rate terms (for example, thermal conductivity, isothermal diffusion coefficient, and Soret coefficient) and X_i are the considered forces of the system. Onsager's reciprocal relations restrict $L_{ij} = L_{ji}$ for $i = j$. For the case of thermal diffusion, the force terms are the gradients in chemical potential μ and temperature T, that is:

$$X_1 = -\nabla\mu \tag{2}$$

$$X_2 = -\nabla T \tag{3}$$

The coupling of the mass and heat provides the following two flux relations:

$$J_{mass} = -D\frac{\partial C}{\partial x} - D\sigma C\frac{\partial T}{\partial x} \tag{4}$$

$$J_{heat} = -D_D CT\frac{\partial C}{\partial x} - \kappa\frac{\partial T}{\partial x} \tag{5}$$

where D is the isothermal diffusion coefficient, C is the concentration of the chemical species, x is the usual one-dimensional coordinate, σ is the Soret coefficient, D_D is the Dufour coefficient, and κ is related to the thermal conductivity. The Soret coefficient is usually defined as the ratio of the thermal diffusion coefficient D_T to the isothermal diffusion coefficient:

$$\sigma = D_T / D \tag{6}$$

Note that these equations assume the system to be static with no convective mass or heat transfer. Equations (4) and (5) contain, respectively, the familiar Fickian diffusion and heat flow terms as diagonal components. However with the coupling of forces, two off-diagonal terms are required to describe the total mass or heat flux. The Dufour term describes the reciprocal process relative to thermal diffusion and represents the transfer of heat associated with a compositional gradient (Rastogi and Yadava, 1969; Mortimer and Eyring, 1980).

To consider the mass flux only of a thermal diffusion system, equation (4) can be directly solved for steady state conditions. By setting equation (4) to zero, the isothermal diffusive flux is equal to the negative of the thermal diffusive flux, or:

$$\frac{\partial C}{\partial x} = -\sigma C\frac{\partial T}{\partial x} \tag{7}$$

Therefore, at steady state the Soret coefficient can be easily obtained by integrating equation (7) to give the following expression:

$$\sigma = -\frac{d\ln C}{dT} \tag{8}$$

A plot of ln C versus T will provide a curve with a slope equivalent to the Soret coefficient. In this case, thermal diffusion will separate, or fractionate, a component to either end of the system, however, compositional gradients which are created will tend to be homogenized by the isothermal diffusion process. By convention, σ is a positive value for transport down the thermal gradient; that is, enrichment of a chemical component occurs at the cold end of the system. The result at steady state, assuming a linear temperature gradient, is a linear compositional gradient. A steady state analysis was utilized by Seyfried and Thornton (1982) and Thornton and Seyfried (1983) in their examination of pore fluids in sediments where temperatures across large reaction zones were measured. However, in the steady state case it is difficult to sort out all of the contributing effects which can alter the concentration distribution. Also, Soret steady state, sometimes referred to as Soret equilibrium, is often jeopardized by remixing through convective processes. For such cases, it is important to examine the evolution of the system toward the steady state condition.

In modeling the transient case, it is necessary to examine equation (4) in light of the following continuity-of-mass equation with t representing time of the process:

$$\frac{\partial C}{\partial t} = -\frac{\partial J}{\partial x} \tag{9}$$

Combining these equations, the general time-dependent partial differential equation is obtained:

$$\frac{\partial C}{\partial t} = \frac{\partial}{\partial x}\left(D\frac{\partial C}{\partial x} + D\sigma C\frac{\partial T}{\partial x}\right) \tag{10}$$

If a linear temperature gradient is imposed on the system, equation (10) can be simplified with the removal of one of its differential cross terms to:

$$\frac{\partial C}{\partial t} = D\frac{\partial^2 C}{\partial x^2} + D\sigma C\frac{\partial T}{\partial x}\frac{\partial C}{\partial x} \qquad (11)$$

With appropriate boundary conditions, usually zero mass flux, and with an initially homogeneous system, equation (11) can be readily solved (Bierlein, 1955; DeGroot and Mazur, 1962). However, there are limits (at small time values) where only approximate analytical solutions are available. In addition, restrictions are imposed by assumptions of the temperature and compositional dependency of the necessary physical property terms (for example, solution density). Korchinsky and Emery (1967) and Tishchenko (1984) discuss some of the limits imposed by the analytical solutions to the non-steady state equations. Graphical representations of the analytical solutions are presented below for the modeling of the Soret experiments.

In all of the analytical solutions, a common characteristic time of steady state attainment results. This time t_{ss} is expressed by the following relationship for the attainment of 98% of the steady state solution:

$$t_{ss} = \frac{4a^2}{\pi^2 D} \qquad (12)$$

The term a represents the length of the system. Interestingly, the time to reach steady state is inversely proportional to the isothermal diffusion coefficient. Nowhere else does the diffusion coefficient occur in the analytical solutions except in the time decay term.

Application of the preceding theory to the thermal diffusion experiment and the determination of Soret coefficients is discussed in the Results section. However, because of the lack of a general model describing the experimental Soret process, a useful numerical model was developed (Cygan and Carrigan, 1992). The numerical solution is used to supplement the analytical solutions and to investigate the effect of non-linear thermal profiles and inhomogeneous initial compositions. The model utilizes an implicit central difference solver which incorporates a Gauss elimination scheme. The one- dimensional thermal diffusion model provides a solution to equation (10) for the case of an evolving

thermal field. Figure 4 presents the evolution of a thermal profile expected in the early stages of the thermal diffusion experiment as heat is conductively transferred across the Soret cavity. The thermal conduction model of Carslaw and Jaeger (1959) was used employing fixed temperatures at the boundaries of the system. The results of the corresponding compositions for the six time periods are presented in Figure 5. Approximate values for the transport parameters (Soret and isothermal diffusion coefficients) of a 0.5 N NaCl solution at 40°C were chosen for input in the model.

Most significant in this numerical result is the initial early stage of the thermal field evolution where large temperature gradients occur at the cell margins. This results in a large flux of material near the margins, but which is restricted in advancing across the cell where the smaller temperature gradients occur. The result is a temporary reversal of enrichment/depletion that would be expected for a fixed linear temperature profile. The extent of the reversal as predicted by this numerical model is beyond the sensitivity of the present experimental technique. Ultimately, the temperature profile becomes linear (thermal steady state) and the concentration profile continues to evolve to its own linear steady state. The middle and late stages of this system (Figure 5) exhibit the compositional profile for times leading to a steady state linear distribution after 4 hours. This final profile represents the solution to the steady state equation (equation (7)). Note that the maximum extent of Soret fractionation at steady state is very limited and is only on the order of 3% of the original composition.

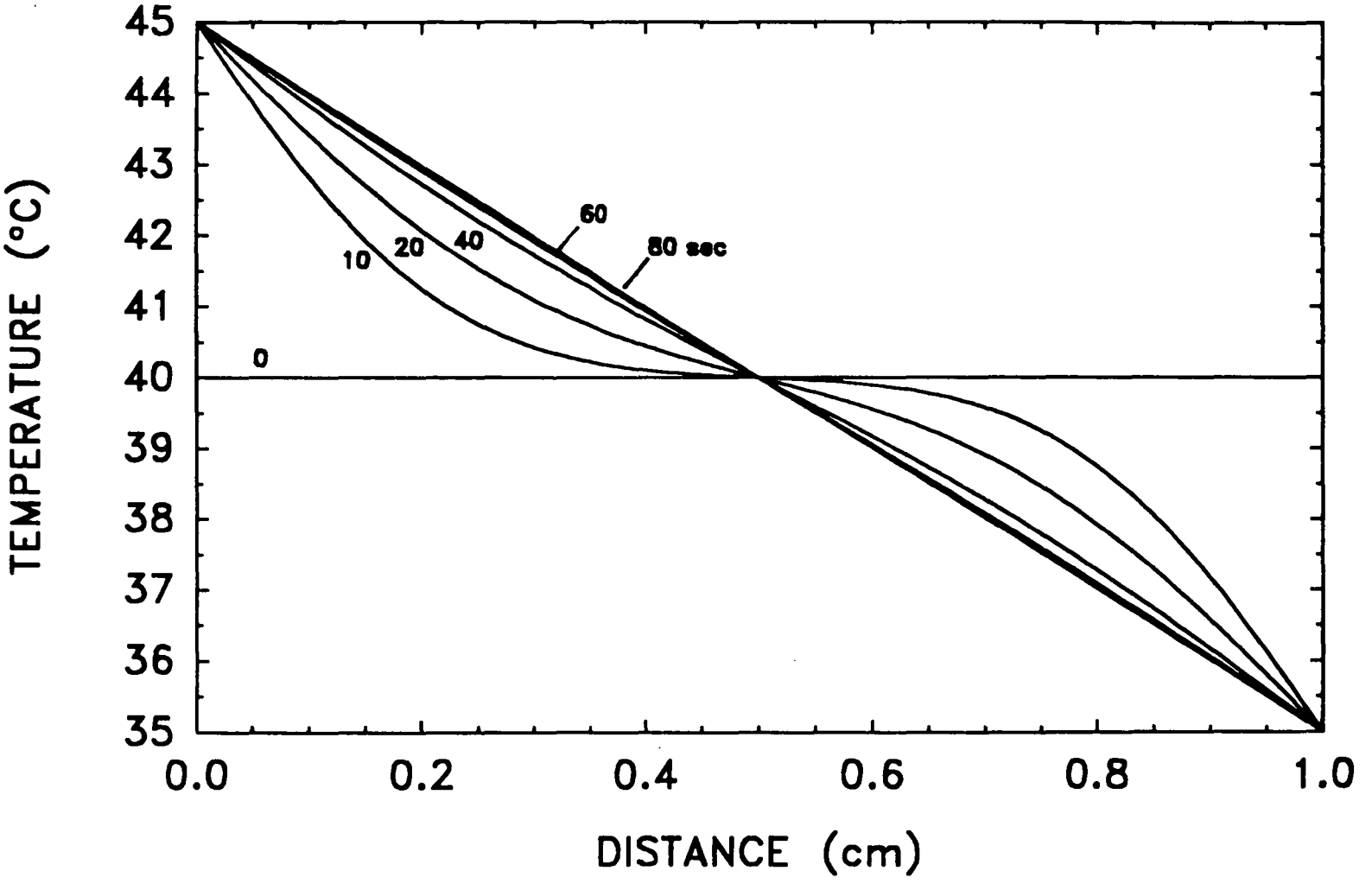

Figure 4. Evolution of a temperature profile by thermal conduction for a 1 cm Soret cell with an isothermal initial state and fixed boundary temperatures. Analytical solution taken from Carslaw and Jaeger (1959).

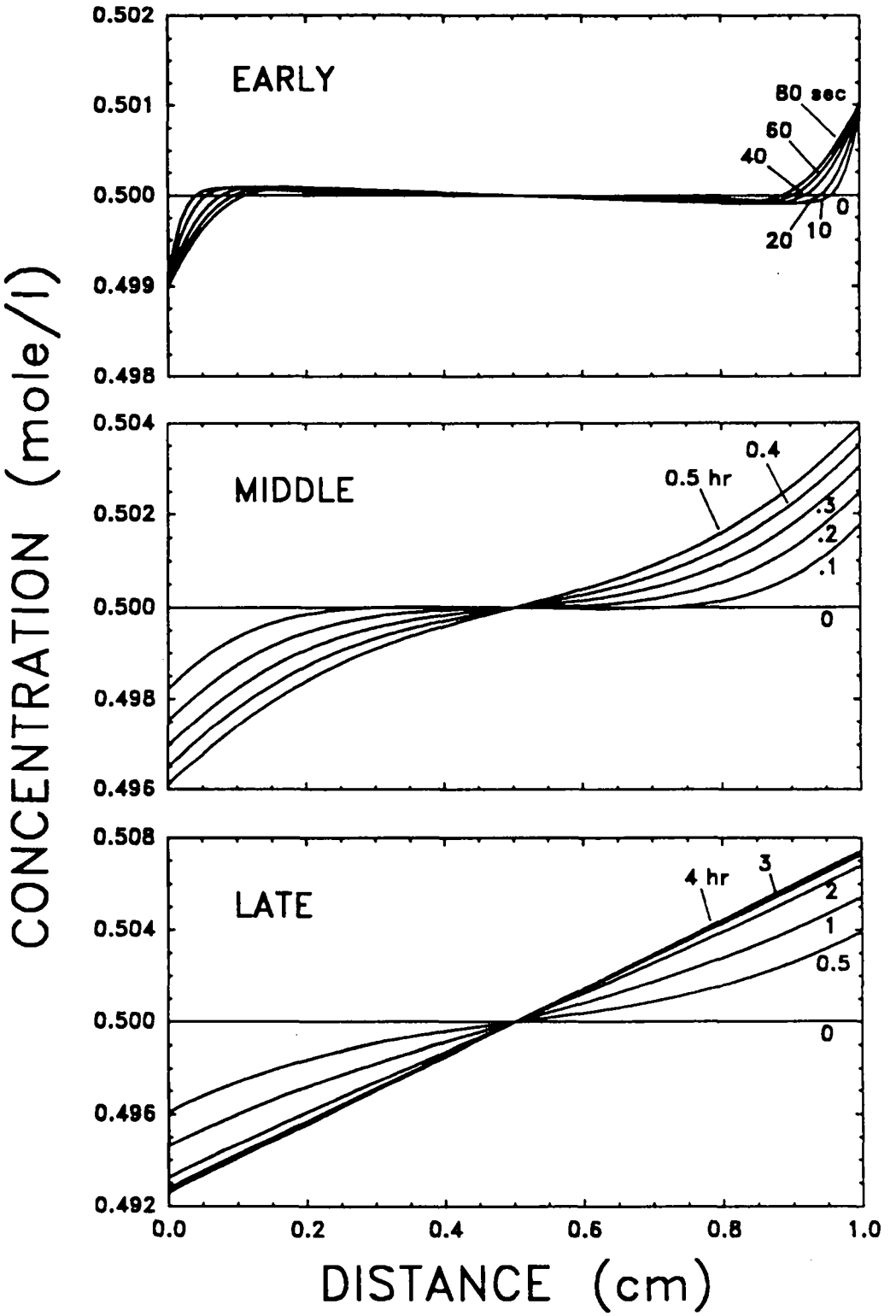

Figure 5. Evolution of compositional profile by thermal diffusion for a 1 cm Soret cell at three different stages of development corresponding to the temperature behavior presented in Figure 4. From Cygan and Carrigan (1992).

EXPERIMENTAL APPROACH

In order to experimentally derive the values of Soret coefficients at elevated temperatures and at high ionic strengths, a conductimetric technique was chosen. The experimental design is based upon the original concept developed by Chipman (1926) and extended by Agar and Turner (1960) for the measurement of Soret and isothermal diffusion coefficients of dilute electrolyte solutions. The approach utilizes the measurement of conductance change of solutions as a function of time. Essentially, electrodes are positioned at either extreme of the so-called "Soret cell" with a common tap electrode wire positioned at the exact center of the cell. A thermal gradient is externally imposed upon the cell such that the higher temperature is maintained at the upper electrode region in order to prevent thermal buoyancy convection. This conductimetric technique was successfully used to measure other dilute aqueous systems (Snowdon and Turner, 1960a, 1960b; Sagert and Breck, 1961) and more concentrated solutions (Price, 1961; Hawksworth *et al.*, 1977; Lobo and Teixeira, 1982). However, the most successful set of experiments which utilized the conductimetric technique were completed by Caldwell (1973, 1974) and Caldwell and Eide (1981). In these recent studies, electrolytes of high ionic strength approaching sea water compositions (for example, 0.5 N NaCl) were examined as a function of temperature (0.5°C to 52°C) and pressure (1 atm to 0.73 kbar). Indeed, these are the only reported studies to have examined the Soret process for concentrated NaCl solutions at relatively high temperatures and pressures.

Other experimental approaches utilized in the determination of Soret coefficients include the interferometric, potentiometric, and direct sampling techniques. The interferometric approach depends upon the change of refractive index of a solution with concentration. This Rayleigh interferometry technique was incorporated by Tanner (1927) in the original experimental work on organic solutions and then modified by others (Thomaes, 1951; Tanner, 1953; Longsworth, 1957; Narbekov and Usmanov, 1971; Dulieu, 1981) for a wide range of compositions of aqueous and organic solutions. The potentiometric approach requires a chemical system which can generate an electrochemical potential to be monitored as a function of time (Agar and Breck, 1957). Yow *et al.* (1977), Yow and Lin (1983), and Petit *et al.* (1986) have recently used this

technique with nonisothermal conditions for deriving Soret data of dilute aqueous solutions. The direct sampling technique requires the hand sampling of solution volumes during the evolution of the Soret process. The obvious problem of solution perturbation and vibration prevents this technique from providing any meaningful results (I. M. Chou, pers. comm.).

Other indirect determinations of Soret coefficients have been obtained through a variety of nonisothermal experimental devices. Thermodialysis techniques (Mita *et al.*, 1982) examine electrolyte transport through a thin membrane. Thermogravitational cells (Carrigan and Cygan, 1986) combine Soret transport with thermal buoyancy convection for the separation of solution components. Often referred to as Clusius-Dickel cells, these nonisothermal systems have been recently used to obtain Soret coefficients for NaCl solutions (Gaeta *et al.*, 1982) and components, including sodium and chloride, of an idealized seawater composition (Caldwell and Eide, 1985). Several of the difficulties in deriving Soret data from this last approach are discussed by Velarde *et al.* (1982) and Henry and Roux (1983). Uncontrolled convection in the vertical columns seldom provides agreement of the derived Soret coefficients with conventionally measured values (Legros *et al.*, 1985; Henry *et al.*, 1987).

After reviewing the variety of experimental techniques, the conductimetric method was recognized as an accurate and reproducible approach for the present study. This technique has proven itself to be very useful towards measuring a wide range of solution compositions and can be used for executing Soret experiments at temperatures up to 70°C. The simplicity and ease of modification of a conductimetric Soret cell for automatic data acquisition was considered to be additionally appealing.

The Soret cell assembly (Figure 6) is comprised of a central cell held between two heat reservoirs. This choice of conductimetric cell is an improvement on the original cell design that was effected by thermal convection of the solution (Cygan, 1985). The central cell was made out of a Plexiglas disc and is characterized by a 1 cm diameter by 1 cm long (0.785 ml volume) cavity (Figure 6). Two small-diameter channels leading from the edge of the disc intersect the central cavity. Threaded nylon screws fit the ends of the channels and allow for access into the cavity for the filling solution as well as for the central platinum

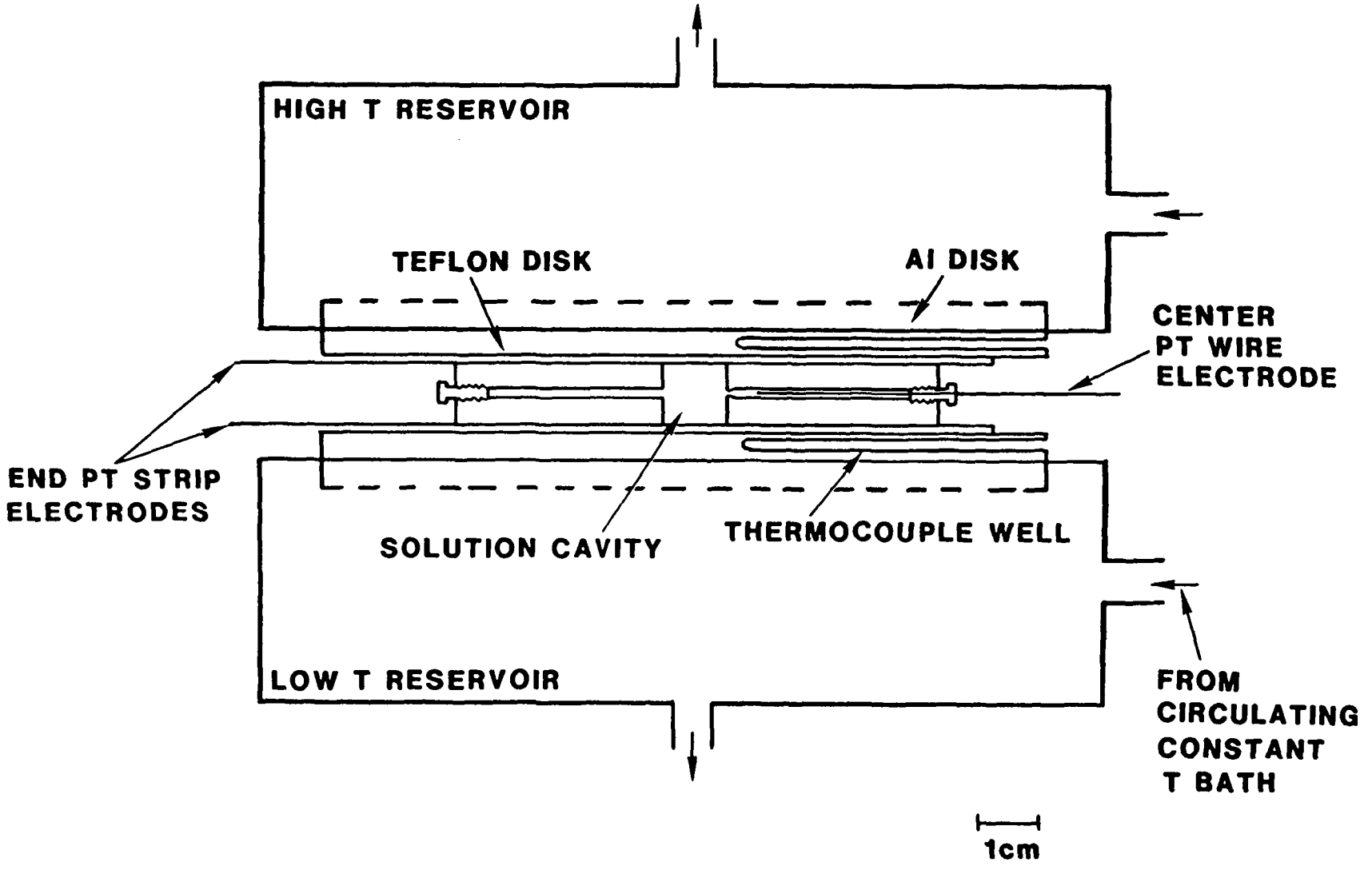

Figure 6. Diagram of the Soret cell assembly. The schematic provides a side view of the cylindrical solution cavity (0.785 ml).

wire electrode. Platinum foil strips, serving as the outer electrodes, cover the Soret cavity and extend out beyond the edge of the disc. Silicone grease is added to the edge of both sides of the cavity to ensure a tight seal. Mylar sheets are placed upon each of the outer platinum electrodes to electrically isolate the Soret cell. This entire assembly is clamped between two isothermal temperature reservoirs with aluminum disks acting as the heat sink material in contact with the mylar insulation (Figure 6). Type T (copper-constantan) thermocouples were housed in sheaths drilled into the lower section of the aluminum disks. The assembly was placed upon a granite slab in order to minimize ambient vibrations during the progress of the Soret run. Two precision constant temperature circulators (Haake model B81) controlling water temperature to 0.05°C are connected to the reservoirs.

A high-precision impedance analyzer (Hewlett-Packard model 4192A) set at a 1 kHz oscillating electrical frequency was utilized for the measurement of the Soret cell conductance. Usually, a low-voltage signal of 0.01 to 0.10 V was used in the measurement in order to minimize any local solution heating and convection. Only the real part of the sample admittance (in siemens) was taken in the measurement. Because of the need to monitor two separate solution conductances, a multiplexer relay/data acquisition control unit (Hewlett-Packard model 3497A) was incorporated. All electrical leads and thermocouples were interfaced through a signal conditioning panel (Data Translation model DT701). All of these units were controlled by a FORTRAN-77 algorithm run by an LSI 11/23 computer (Digital Equipment Corporation). Interfacing was completed by standard IEEE (National Instruments GPIB 11V-1 IEEE) and D/A and A/D (Data Translation) devices.

The run procedure entails filling the Soret cell with the desired solution by syringe through the filling port. Slow filling of this cavity prevented bubbles from forming; however, it was often necessary to remove bubbles by manipulation of the cell and by applying suction with the syringe. Once completed, the Soret cavity was isolated by the threaded screws, and the circulating baths were activated to bring the entire cell to a common low end temperature. It was necessary to loosen the filling port screw to allow for thermal expansion of the solution during this heating period. The entire assembly was leveled using a bubble level such that the Soret cell was in vertical alignment with the expected

hot end above the cold end. The three Soret cell electrodes were attached to the signal conditioning panel and the remainder of the electrical system. The impedance analyzer was calibrated for open and short circuits at this time. Once thermally equilibrated to a common temperature, the temperature of the upper circulator/reservoir was increased to an appropriate run temperature in order to generate the desired thermal gradient across the solution. This was considered the zero time of the experiment, although there was a lag time necessary for the linear temperature gradient to form (see earlier discussion).

The computer program monitored the experiment at this stage by measuring both upper and lower solution conductance (impedance) at given time increments. Usually multiple readings were averaged for both conductance and temperature measurements. Conductance was corrected for temperature effects based upon previously determined calibration curves for the selected solution compositions. (The relative conductance temperature derivatives for NaCl solutions are 0.0148 /deg, 0.0145 /deg, and 0.0143 /deg for, respectively, 0.1, 0.5, and 1.0 N solutions). All collected and reduced data were printed during real time execution and then stored on magnetic disk for future data reduction.

Multiple Soret experiments were completed for three relatively high concentrations of NaCl-H_2O solutions (0.1, 0.5, and 1.0 N NaCl). Soret data were obtained at average temperatures of 40°C and 50°C and for temperature gradients of 10°C/cm and 20°C/cm. These experiments were run for up to seven hours of duration so that the entire transient period of Soret evolution leading up to steady state could be obtained. Normally, measurements were made every two to five minutes during this period to provide the necessary resolution in time.

RESULTS AND DISCUSSION

In order to extract the Soret diffusion coefficients from the conductance data obtained during the experimental run, the analytical model of Bierlein (1955) was utilized. As the conductance values were obtained for the two ends of the cells, the evaluation of the analytical model for the endpoints of the cell was used. The ratio of the hot zone concentration to that of the cold end (which is equivalent to the mole fraction ratio for the solutions of interest) is:

$$\frac{C_{hot}}{C_{cold}} = \frac{1+\frac{1}{2}\sigma\Delta T - \frac{4\sigma\Delta T}{\pi^2}e^{-t/\theta}}{1-\frac{1}{2}\sigma\Delta T + \frac{4\sigma\Delta T}{\pi^2}e^{-t/\theta}} \tag{13}$$

where:

$$\theta = \frac{a^2}{\pi^2 D} \tag{14}$$

ΔT is the temperature difference between end plates of the cell while the concentration subscripts denote the relative temperatures of these end positions. Equation (13) assumes that the mole fraction of the component is much less than one (that is, the solution is relatively dilute). Figure 7 provides a plot of this relationship along with the results of the numerical model and the approximate solution of DeGroot (1947). All of the models presented assume a linear temperature gradient of 10°C/cm. The agreement of the Bierlein and numerical models, except for very early times, supports the use of the former in the modeling of the experimental data.

By equating the ratio of solution conductance to the ratio of concentrations, a direct comparison of the model and experiment can be obtained. This approach allows for the simultaneous fitting of both the Soret and isothermal diffusion coefficients for all experimental values. It provides an improvement over the linearization required in the approach of Snowdon and Turner (1960a) and later by Caldwell (1973). Excessively high values of the isothermal diffusion coefficients suggest a problem with convective remixing of the solution. Values of the NaCl-H_2O diffusion coefficients were taken from Harned and Owen (1958)

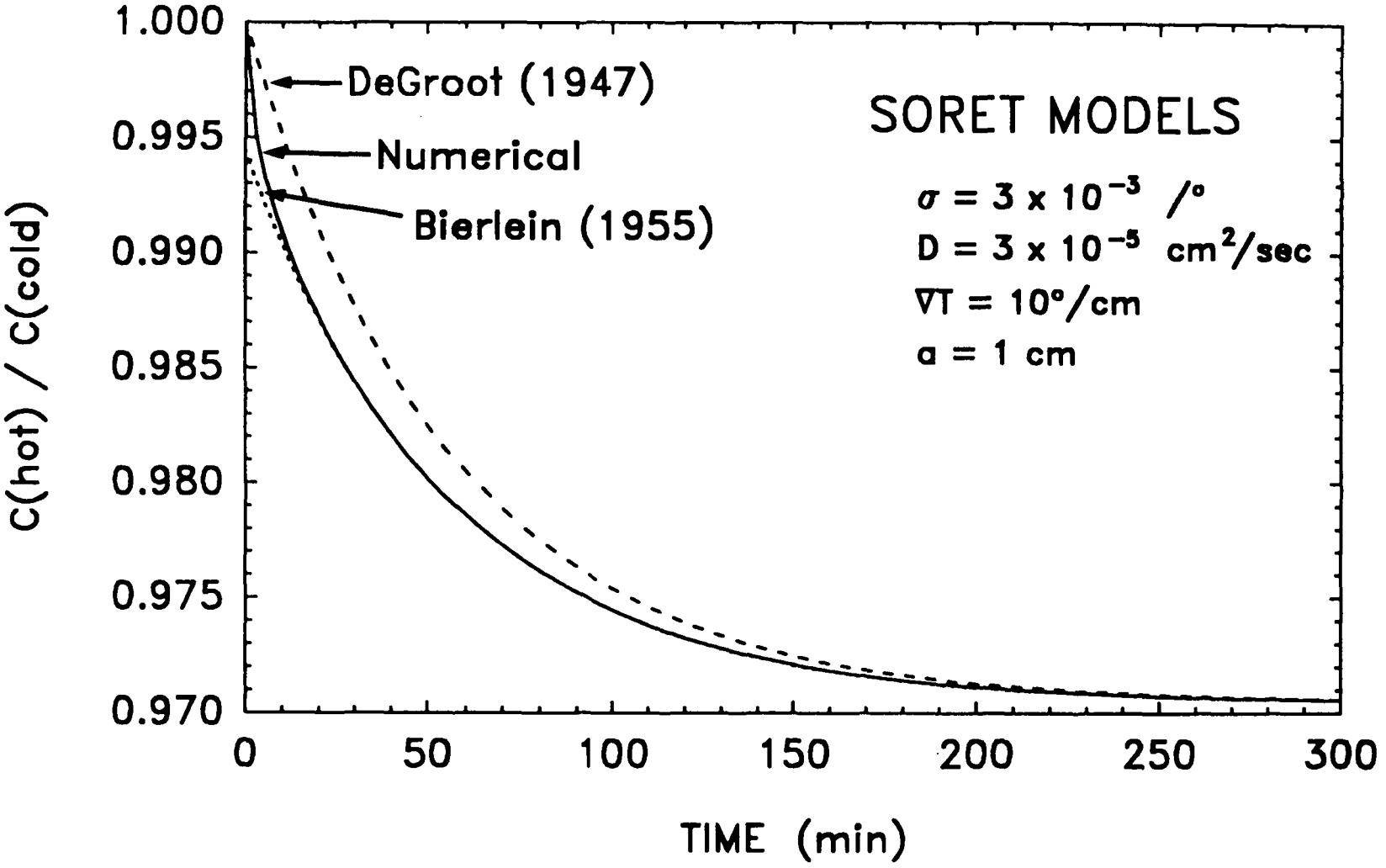

Figure 7. Evolution of the ratio of end concentrations of a Soret cell as a function of time. Analytical solutions of DeGroot (1947) and Bierlein (1955) are presented in addition to the numerical solution. The DeGroot model is an approximate solution. The Bierlein model, although in agreement with the numerical model over most time, fails to predict the initial condition of unit value for the concentration ratio. The extent of Soret separation is denoted by the final steady state concentration ratio, whereas the isothermal diffusion term determines time to reach steady state.

and D. G. Miller (pers. comm.), the latter values for the high temperature runs. It was fairly common to obtain more than an order-of-magnitude difference in these values, however these runs were characterized by fairly flat conductance ratio curves. The difficulty in achieving an acceptable data set was usually generated by considerable drift and variability of the impedance analyzer during the course of the run. The Soret data reported are only for experimental runs which were repeated and had Soret coefficients which were within 25% agreement of each other.

Figure 8 provides a typical plot of the conductance ratio decay during the evolution of the Soret cell solution towards a linear steady state. The results are for a 1 cm Soret cell with the end temperatures maintained at 45°C and 35°C. Multiple curves are presented for the model fits. Note that the numerical model is utilized for the small time values. One estimate of the variability of the Soret coefficient is provided by the additional models about the central curve. As predicted by the models, one expects an immediate, high flux stage at the ends of the Soret cell followed by a gradual approach to steady state. Equation (12) predicts a steady state attainment time of approximately 260 minutes (T = 40°C) which is mirrored in the measured conductance ratio decay.

The results for the successful Soret experiments are presented in Table 1. The Soret coefficients are presented as functions of the three concentrations of NaCl solutions and the mean run temperature. All but one experimental run were completed with a 10°C/cm thermal gradient; the exception being at 20°C/cm. No discernible difference within the estimated uncertainties was noted for the results for the two different gradients (1.0 N NaCl at 40°C). Such thermal gradient dependence is difficult to examine based upon the present theoretical models and the adverse nature of experimentally measuring the Soret effect. Mean temperatures have traditionally been used in the analysis of thermal diffusion with appropriate averaging of solution properties for the half-cells of the Soret assembly. Even with a Soret coefficient independent of the thermal gradient, it is important to reiterate that the mass flux of material by thermal diffusion will be proportional to the magnitude of the thermal gradient.

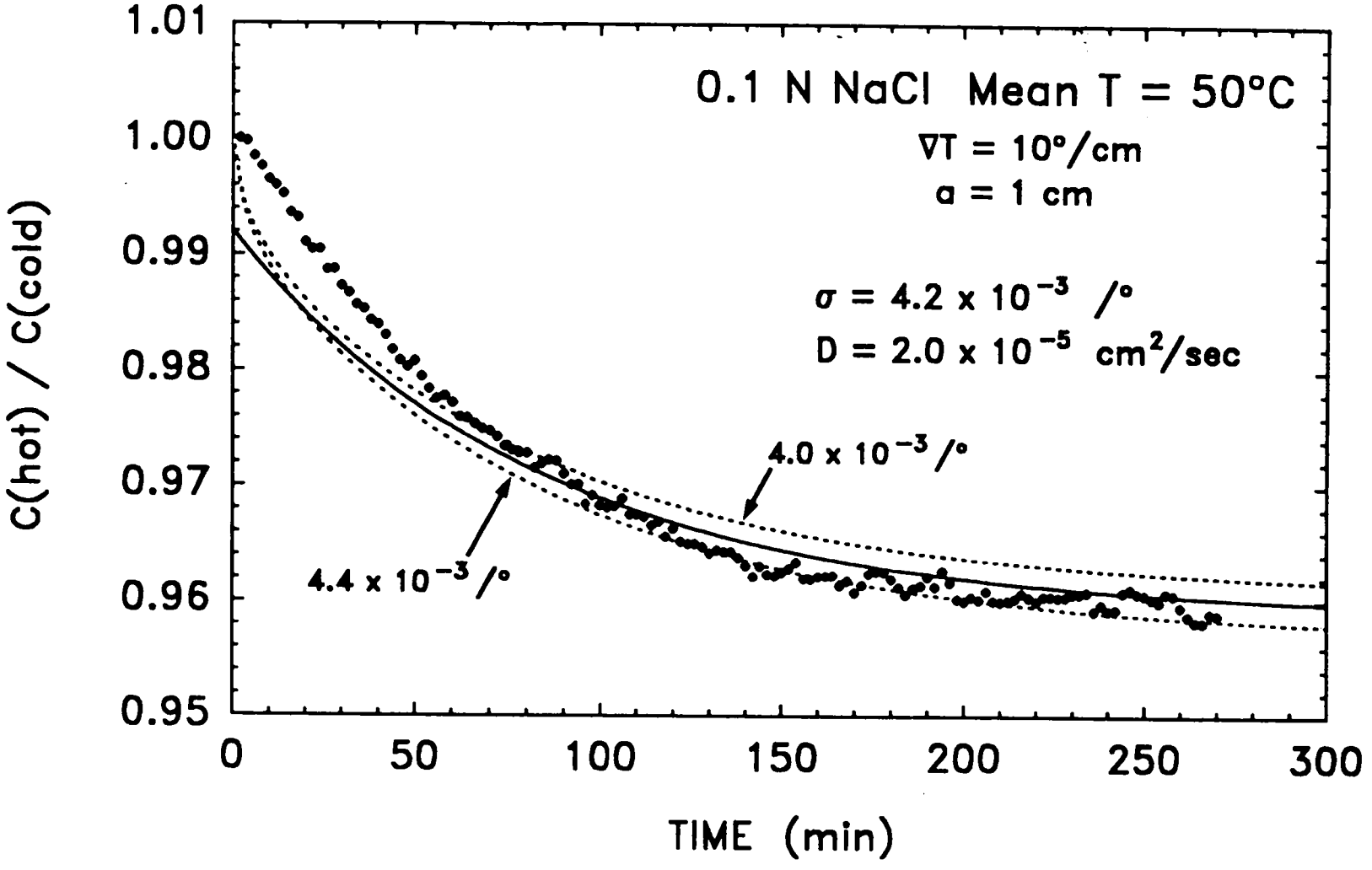

Figure 8. Results of a thermal diffusion run, for a 0.1 N NaCl solution at a mean temperature of 50°C and a thermal gradient of 10°C/cm, in terms of the ratio of cell end concentrations as a function of time. The best fit to the experimental data is provided by the central curve generated by the Bierlein model. Two dotted curves (numerical solutions) demonstrate the evolution of the ratio for bracketed values of the Soret coefficient.

TABLE 1

SORET COEFFICIENTS (x 10^{-3} /deg)
10°C/cm Temperature Gradient

	Mean Temperature	
Solution Concentration	40°C	50°C
0.1 N NaCl	2.00	3.45
	2.50	4.20
0.5 N NaCl	1.25	2.05
	1.40	3.00
	1.80	3.15
1.0 N NaCl	1.05	3.55
	1.65	3.90
	1.90*	

*Observed at 20°C/cm

Figure 9 provides a plot of the temperature dependence of the Soret coefficient for the results of the 0.5 N NaCl determinations from this study along with the best-fit curve of the reliable data from Caldwell (1973). Note that the latter study examined the thermal diffusion response of seawater for a wide range of conditions including near-freezing temperatures and was able to determine a change in sign of the Soret coefficient. NaCl will migrate from the cold region to the hot region at temperatures below 12°C. Trends in the data obtained from the present study exhibit similar temperature effects, although there is some disagreement in the magnitude of the values between studies. There appears to be considerably greater uncertainty present for this study based upon the reproducibility of the data.

Equation (6) defines the Soret coefficient as the ratio of the thermal and isothermal diffusion coefficients. Assuming both processes have similar temperature dependency as described by the usual Stokes-Einstein relation and its direct linear relation between the coefficient and temperature (Cussler, 1984), one would not expect to observe any significant temperature dependence of the Soret coefficient. However, deviations form Stokes-Einstein behavior for either process appear to be significant to create some positive dependency of the observed Soret coefficient with temperature. Nonetheless, for a given range of temperature, the Soret coefficients will increase at a significantly lower rate than that expected of isothermal diffusion coefficients. Certainly for extrapolation to the higher temperatures of the near-field environment expected at a nuclear waste repository, Soret values would not increase by more than a factor of three.

Figure 10 combines the lower temperature (approximately 25°C) data from several studies (Agar and Turner, 1960; Snowdon and Turner, 1960a, 1960b; Chanu, 1967) and the high temperature (40°C and 50°C) results of the present research. The previous studies are represented by a general curve which is characterized by a pronounced minimum at approximately 0.5 N concentration. This minimum is very much representative of other electrolyte aqueous salts (Chanu, 1967; Leaist, 1990). The trend in the Soret values obtained in the present study is similar to the general curve of these data. There is also a shift of the data towards larger Soret coefficient values due to the temperature effect. This type of concentration dependency is similar to that observed for isothermal

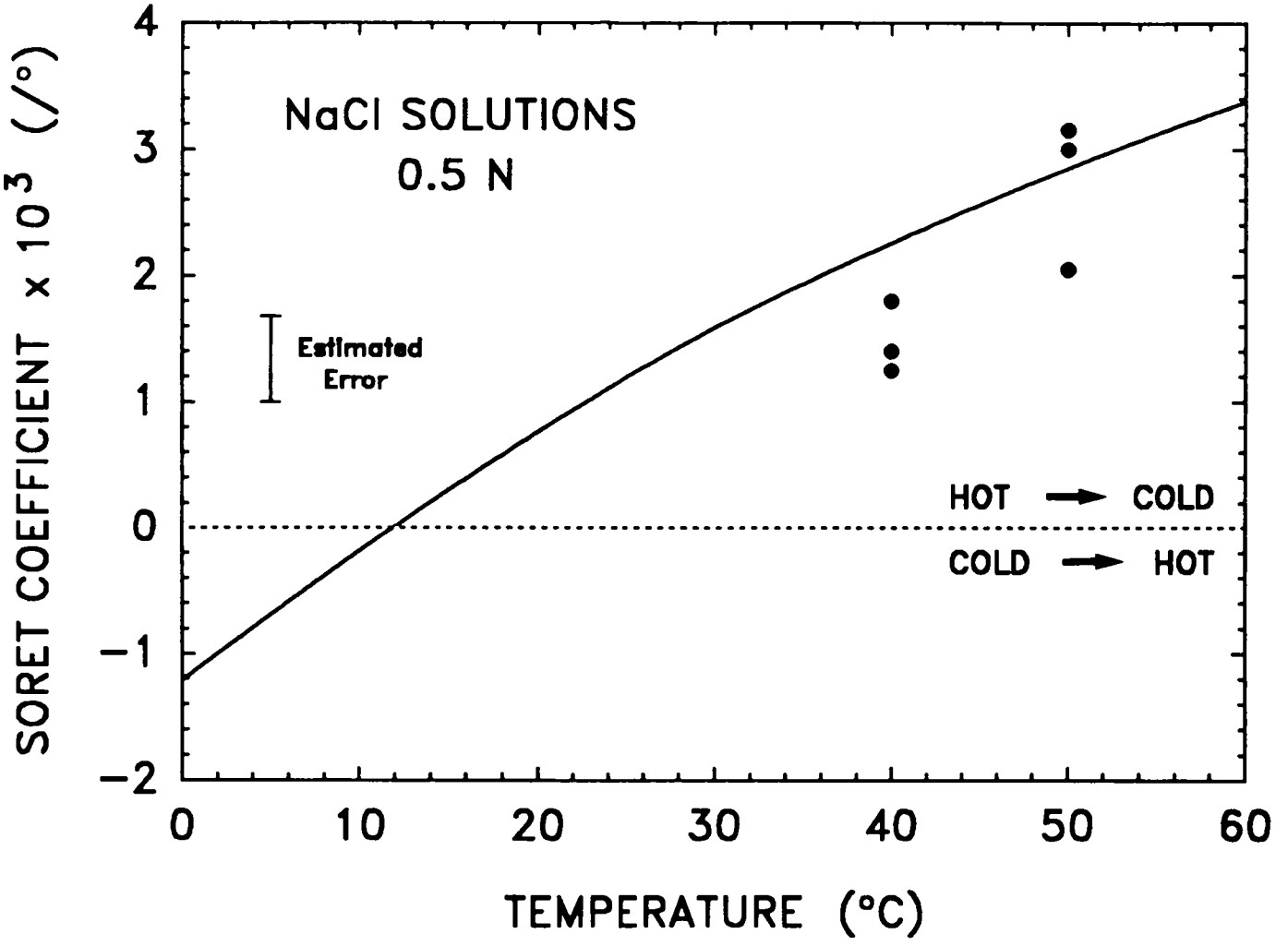

Figure 9. Soret coefficients for a 0.5 N NaCl solution as a function of temperature. The solid curve provides the best fit of the data from Caldwell (1973) for a solution of oceanic concentration.

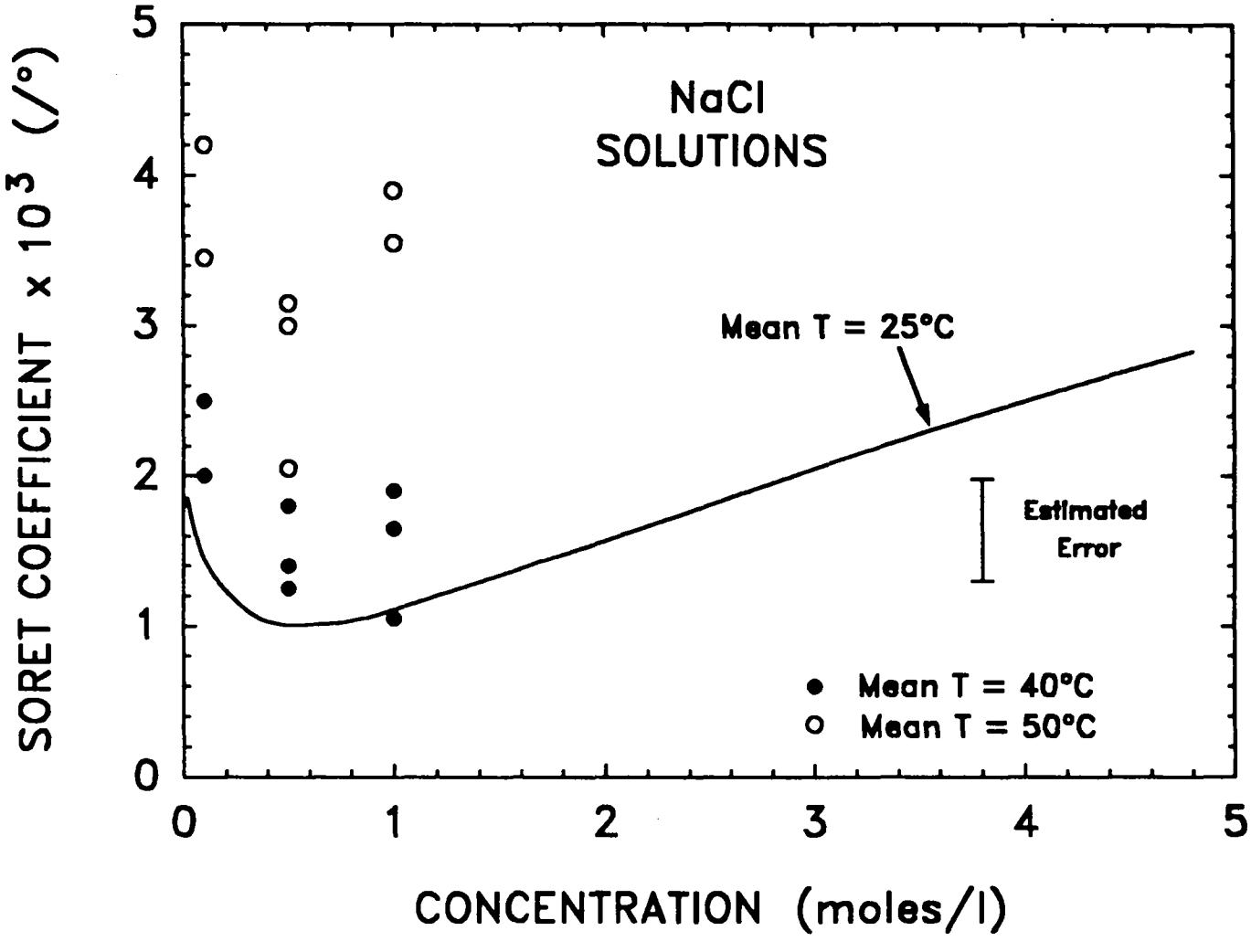

Figure 10. Soret coefficients for NaCl solutions as a function of concentration. The solid curve denotes the best fit to values obtained from a variety of experimental studies performed on solutions at a mean temperature of 25°C. The data points represent the results of this study and are for data obtained at mean temperatures of 40°C and 50°C.

diffusion coefficients and the contribution of activity coefficients in describing the solute concentration and activity.

CONCLUSION

The experimental results for the Soret coefficients are variable, but suggest a trend with NaCl concentration that is consistent with electrolyte solution behavior. The temperature dependence of the Soret coefficients is in approximate agreement with previous measurements obtained using other techniques. In general, the Soret coefficient values are best interpreted based on the expansion of the fluid inclusion migration fields that are presented in Figures 2 and 3. The high temperature values for σ at 1.0 N NaCl concentration suggest an expansion of the migration field to smaller inclusion sizes, which for a single halite crystal at these conditions, approach a dimension of one micron. The corresponding fluid inclusion size for the polycrystalline material, where grain boundaries retard the migration, is approximately 10 microns.

Although the Soret results obtained in the present study provide additional data for high temperature applications in nuclear waste isolation, considerably more experimentation and new equipment design are required in order to obtain data at temperatures greater than 80°C. The experimental approach utilized in this study is limited in that respect. The almost immeasurable nature of the thermal diffusion process for the brines as examined in the laboratory, suggests that this effect will be insignificant (outside of fluid inclusion migration) in most rock-water interactions associated with a rocksalt nuclear waste repository. Other effects, such as convective fluid transport, pressure solution, and groundwater flow, will be orders-of-magnitude more important in evaluating the critical nature of brine migration, waste canister corrosion, and the potential for leaching radioisotopes from waste repositories.

REFERENCES

Agar, J. N. (1960) The rate of attainment of Soret equilibrium. **Transactions of the Faraday Society**, 56, 776-787.

Agar, J. N. and Breck, W. G. (1957) Thermal diffusion in non-isothermal cells. **Transactions of the Faraday Society**, 53, 167-178.

Agar, J. N. and Turner, J. C. R. (1960) Thermal diffusion in solutions of electrolytes. **Proceedings of the Royal Society**, A255, 307-330.

Bierlein, J. A. (1955) A phenomenological theory of the Soret diffusion. **Journal of Chemical Physics**, 23, 10-14.

Bischoff, J. L. and Rosenbauer, R. J. (1989) Salinity variations in submarine hydrothermal systems by layered double-diffusive convection. **Journal of Geology**, 97, 613-623.

Caldwell, D. R. (1973) Thermal and Fickian diffusion of sodium chloride in a solution of oceanic concentration. **Deep-Sea Research**, 20, 1029-1039.

Caldwell, D. R. (1974) The effect of pressure on thermal and Fickian diffusion of sodium chloride. **Deep-Sea Research**, 21, 369-375.

Caldwell, D. R. and Eide, S. A. (1981) Soret coefficient and isothermal diffusivity of aqueous solutions of five principal salt constituents of seawater. **Deep-Sea Research**, 28A, 1605-1618.

Caldwell, D. R. and Eide, S. A. (1985) Separation of seawater by Soret diffusion. **Deep-Sea Research**, 32, 965-982.

Carnahan, C. L. (1984) Thermodynamic coupling of heat and matter flows in near-field regions of nuclear waste repositories. **Materials Research Society Symposium Proceedings**, 26, 1023-1030.

Carrigan, C. R. and Cygan, R. T. (1986) Implications of magma chamber dynamics for Soret-related fractionation. **Journal of Geophysical Research**, 91, 11451-11461.

Carslaw, H. S. and Jaeger, J. C. (1959) **Conduction of Heat in Solids**, Oxford University Press, Oxford, 510 pp.

Chanu, J. (1967) Thermal diffusion of halides in aqueous solution. In **Advances in Chemical Physics**, vol. 13, edited by I. Prigogine, pp. 349-367, Interscience, London.

Chipman, J. (1926) The Soret effect. **Journal of the American Chemical Society**, 48, 2577-2589.

Chou, I. M. (1982a) Migration rates of brine inclusions in single crystals of NaCl. In **Scientific Basis for Nuclear Waste Management**, vol. 6, edited by S. V. Topp, pp. 303-307, Plenum Press, New York.

Chou, I. M. (1982b) Remarks on "The migration of brine inclusions in salt". **Nuclear Technology**, 63, 507-509.

Costeséque, P. (1985) Sur la migration des éléments par thermodiffusion: Etat et perspectives d'un modéle géochimique. **Bulletin de Minéralogie**, 108, 305-32.

Cussler, E. L. (1984) **Diffusion: Mass Transfer in Fluid Systems**, Cambridge University Press, Cambridge, 525 pp.

Cygan, R. T. (1985) Soret diffusion processes in aqueous sodium chloride solutions. (abstract) **Geological Society of America Abstracts with Programs**, 17, 557.

Cygan, R. T. and Carrigan, C. R. (1992) Time-dependent Soret transport: Applications to brine and magma. **Chemical Geology**, 95, 201-212.

DeGroot, S. R. (1947) Détermination des constantes de diffusion thermique et de diffusion ordinaire: A partir des résultats expérimentaux de l'effet Soret pur. **Le Journal de Physique et le Radium**, 8, 129-134.

DeGroot, S. R. and Mazur, P. (1962) **Non-Equilibrium Thermodynamics**, North-Holland, Amsterdam, 510 pp.

Denbigh, K. G. (1952) The heat of transport in binary regular solutions. **Transactions of the Faraday Society of London**, 48, 1-8.

Dickey, P. A. (1966) Patterns of chemical composition in deep subsurface waters. **Bulletin of the American Association of Petroleum Geologists**, 50, 2472-2478.

Dickey, P. A. (1969) Increasing concentration of subsurface brines with depth. **Chemical Geology**, 4, 361-370.

Dulieu, B. (1981) A propos de l'influence de la convection sur la mesure de l'effet Soret: Le cas d'un defaut d'horizontalite; Deuxieme partie: Resultats experimentaux. **Journal de Chimie Physique**, 78, 199-201.

Furry, W. H., Jones, R. C., and Onsager, L. (1939) On the theory of isotope separation by thermal diffusion. **Physical Review**, 55, 1083-1095.

Gaeta, F. S., Perna, G., Scala, G., and Belucci, F. (1982) Nonisothermal matter transport in sodium chloride and potassium chloride aqueous solutions: 1. Homogeneous system (thermal diffusion). **Journal of Physical Chemistry**, 86, 2967-2974.

Ghadekar, S. R. and Deshmukh, B. T. (1982) Microstructures, thermal diffusion and decomposition studies in the two phase solution grown crystals of NaCl and KCl. **Bulletin of Material Science**, 4, 477-481.

Harned, J. and Owen, R. (1958) **The Physical Chemistry of Electrolytic Solutions**, Reinhold, New York, 700 pp.

Hawksworth, W. A., Stiff, A. J., and Wood, C. D. (1977) Thermal diffusion studies in dilute aqueous and non-aqueous electrolyte solutions. **Electrochimica Acta**, 22, 1065-1069.

Henry, D. and Roux, B. (1983) Stationary and oscillatory instabilities for mixture subjected to Soret effect in vertical cylinder with axial temperature gradient. **European Space Agency Special Publication**, ESPUD4, 145-152.

Henry, D., Roux, B., and Burke, W. R. (1987) Numerical study of the perturbation of Soret experiments by three-dimensional buoyancy driven flows. **Proceedings of the Sixth European Symposium on Material Science under Microgravity Conditions**, ESA-SP-256.

Jenks, G. H. (1979) Effects of temperature, temperature gradients, stress and irradiation on migration of brine inclusions in a salt repository. **Oak Ridge National Laboratory, ORNL-5526**, unpublished, 72 pp.

Jenks, G. H. and Claiborne, H. C. (1981) Brine migration in salt and its implications in the geologic disposal of nuclear waste. **Oak Ridge National Laboratory, ORNL- 5818**, unpublished, 164 pp.

Jones, R. C. and Furry, W. H. (1946) The separation of isotopes by thermal diffusion. **Reviews of Modern Physics**, 18, 151-224.

Korchinsky, W. J. and Emery, A. H. (1967) The forgotten effect in thermal diffusion. **American Institute of Chemical Engineers Journal**, 13, 224-230.

Krause, W. B. and Loken, M. C. (1981) Thermomechanical modeling of a thin-disk rock salt core sample exposed to temperature gradients. **Sandia National Laboratories, Topical Report RSI-0113**, unpublished, 24 pp.

Leaist, D. G. (1990) Soret coefficients of mixed electrolytes. **Journal of Solution Chemistry**, 19, 1-10.

Legros, J. C., Goemaere, P., and Platten, J. K. (1985) Soret coefficient and the two-component Benard convection in the benzene-methanol system. **Physical Review A**, 32, 1903-1905.

Lobo, V. M. M. and Teixeira, M. H. S. F. (1982) Soret coefficients of some polyelectrolytes. **Electrochimica Acta**, 27, 1145-1147.

Longhurst, G. R. (1985) The Soret effect and its implications for fusion reactors. **Journal of Nuclear Materials**, 131, 61-69.

Longsworth, L. G. (1957) The temperature dependence of the Soret coefficient of aqueous potassium chloride. **Journal of Physical Chemistry**, 61, 1557-1562.

Mita, D. G., Bellucci, F., Cutull, M. G., and Gaeta, F. S. (1982) Nonisothermal matter transport in sodium chloride and potassium chloride aqueous solutions: 2. Heterogeneous membrane system (thermodialysis). **Journal of Physical Chemistry**, 86, 2975-2982.

Mizushina, T. and Ito, R. (1963) Thermal diffusion in binary liquid mixtures. **Industrial Engineering and Chemical Fundamentals**, 2, 102-106.

Mortimer, R. G. and Eyring, H. (1980) Elementary transition state theory of the Soret and Dufour effects. **Proceedings of the National Academy of Sciences of the USA**, 77, 1728-1731.

Narbekov, A. I. and Usmanov, A. G. (1971) Analysis of thermodiffusion in liquids. **Journal of Engineering Physics**, 21, 1052-1056.

Olander, D. R., Machiels, A. J., Balooch, M., and Yagnik, S. J. (1982) Thermal gradient migration of brine inclusions in synthetic alkali halide single crystals. **Journal of Applied Physics**, 53, 669-681.

Petit, C. J., Hwang, M. H., and Lin, J. L. (1986) The Soret effect in dilute aqueous alkaline earth and nickel chloride solutions at 25 C. **International Journal of Thermophysics**, 7, 687-697.

Pigford, T. H. (1982) Migration of brine inclusions in salt. **Nuclear Technology**, 56, 93-101.

Powers, J. E. (1962) Thermal diffusion. In **New Chemical Engineering Separation Techniques**, edited by H. M. Schoen, pp. 1-98, Interscience, New York.

Price, C. D. (1961) Thermal diffusion in solutions of electrolytes. **Office of Aerospace Research, US Air Force, Technical Report AD 276 280**, unpublished, 32 pp.

Rastogi, R. P. and Yadava, B. L. S. (1969) Dufour effect in liquid mixtures. **Journal of Chemical Physics**, 51, 2826-2830.

Reuther, H. (1984) Contribution to the thermotransport in silicate glasses. **Physica Status Solidi**, 83, 173-178.

Roedder, E. and Belkin, H. E. (1980) Thermal gradient migration of fluid inclusions in single crystals of salt form the Waste Isolation Pilot I Plant Site (WIPP). In **Scientific Basis for Nuclear Waste Management**, vol. 2, edited by C. J. M. Northrup, pp. 453-464, Plenum Press, New York.

Rothmeyer, M. (1980) The Soret effect and salt-gradient solar ponds. **Solar Energy**, 25, 567-568.

Sagert, N. H. and Breck, W. G. (1961) Thermal diffusion and ammonium salts in aqueous solution. **Transactions of the Faraday Society**, 57, 436-446.

Schott, J. (1983) Thermal diffusion and magmatic differentiation: A new look at an old problem. **Bulletin de Minéralogie**, 106, 247-262.

Seyfried, W. and Thornton, E. C. (1982) Experimental studies of water-rock interaction processes in a thermal gradient: Thermal diffusion and sediment-seawater interaction in the near field environment. **Sandia National Laboratories, Annual Progress Report**, unpublished, 55 pp.

Snowdon, P. N. and Turner, J. C. R. (1960a) The Soret effect in some 0.01 normal aqueous electrolytes. **Transactions of the Faraday Society**, 56, 1409-1418.

Snowdon, P. N. and Turner, J. C. R. (1960b) The concentration dependence of the Soret effect. **Transactions of the Faraday Society**, 56, 1812-1819.

Tanner, C. C. (1927) The Soret effect. Part I. **Transactions of the Faraday Society**, 23, 75-95.

Tanner, C. C. (1953) The Soret effect. Part II. **Transactions of the Faraday Society**, 49, 611-619.

Thomaes, G. (1951) Recherches sur la thermodiffusion en phase liquide: L'effet Soret élémentaire. **Physica**, 17, 885-898.

Thornton, E. C. and Seyfried, W. E. (1983) Thermodiffusional transport in pelagic clay: Implications for nuclear waste disposal in geological media. **Science**, 220, 1156-1158.

Tishchenko, P. Y. (1984) Soret equilibrium in a multi-component electrolyte. **Russian Journal of Physical Chemistry**, 58, 129-130.

Tsang, C. F., Noorishad, J., and Wang, J. S. Y. (1983) A study of coupled thermomechanical, thermohydrological and hydromechanical processes associated with a nuclear waste repository in a fractured rock medium. **Materials Research Society Symposium Proceedings**, 15, 515-522.

Velarde, M. G. and Garcia-Ybarra, P. L. (1982) A model describing Soret diffusion and convective instability in a closed vertical column. **Journal of Non-Equilibrium Thermodynamics**, 7, 253-258.

Wada, K., Suzuki, A., Sato, H., and Kikuchi, R. (1985) Soret effect in solids. **Journal of Physics and Chemistry of Solids**, 46, 1195-1205.

Yow, H. K., Chakraborty, B. P., and Lin, J. (1977) Thermal diffusion of alkali chlorides in H_2O and D_2O. **Electrochimica Acta**, 22, 1013-1019.

Yow, H. and Lin, J. (1983) Thermal diffusion of lanthanide chlorides. **Journal of Solution Chemistry**, 12, 487-502.

DISTRIBUTION LIST

Charles R. Carrigan
Lawrence Livermore National Laboratory
Earth Sciences Department, L-206
7000 East Avenue
Livermore, CA 94550

I-Ming Chou
U.S. Geological Survey
959 National Center
Reston, VA 22092

Terry M. Gerlach
U.S. Geological Survey
Cascades Volcano Observatory
5400 MacArthur Blvd.
Vancouver, WA 98661

Glenn D. Jarrell (5)
ManTech Environmental Technology Inc.
Corvallis, OR 87333

Antonio C. Lasaga
Department of Geology and Geophysics
Yale University
New Haven, CT 06511

C. E. Lesher
Lamont Doherty Geological Observatory
Palisades, NY 10964

William C. Luth
U.S. Department of Energy
Office of Basic Energy Sciences
Geosciences Research, ER-15
Washington, D.C. 20585

Richard M. Mitterer
U.S. Department of Energy
Office of Basic Energy Sciences
Geosciences Research, ER-15
Washington, D.C. 20585

J. Donald Rimstidt
Department of Geological Sciences
Virginia Polytechnic and State Institute
Blacksburg, VA 24061

David Walker
Lamont Doherty Geological Observatory
Palisades, NY 10964

1513	D. F. McTigue
6000	D. L. Hartley
6100	P. J. Hommert, Actg.
6111	J. C. Dunn
6112	D. A. Northrup
6113	J. K. Linn
6114	M. W. Scott
6116	M. C. Walck
6117	W. R. Wawersik
6117	D. H. Zeuch
6118	R. T. Cygan (20)
6118	J. L. Krumhansl
6118	C. L. Stein
6118	H. R. Westrich
6119	E. D. Gorham
6121	J. R. Tillerson
6300	D. E. Miller
6302	T. E. Blejwas
6341	A. L. Stevens
6342	D. R. Anderson
6343	T. M. Schultheis
6345	R. C. Lincoln
7141	Technical Library (5)
7151	Technical Publications (1)
7613-2	Document Processing for DOE/OSTI (10)
8523-2	Central Technical Files